Auxiliary Master Equation for Nonequilibrium Dual-Fermion Approach

Feng Chen, Guy Cohen, and Michael Galperin

Auxiliary master equation for nonequilibrium dual-fermion approach

Feng Chen,[1] Guy Cohen,[2, 3] and Michael Galperin[4, *]

[1]*Department of Physics, University of California San Diego, La Jolla, CA 92093, USA*
[2]*The Raymond and Beverley Sackler Center for Computational Molecular and Materials Science, Tel Aviv University, Tel Aviv 69978, Israel*
[3]*School of Chemistry, Tel Aviv University, Tel Aviv 69978, Israel*
[4]*Department of Chemistry & Biochemistry, University of California San Diego, La Jolla, CA 92093, USA*

We introduce an auxiliary quantum master equation dual fermion method (QME-DF) and argue that it presents a convenient way to describe steady-states of correlated impurity models. The scheme yields an expansion around a reference that is much closer to the true nonequilibrium state than that in the original dual fermion formulation. In steady-state situations, the scheme is numerically inexpensive and avoids time propagation. The Anderson impurity model is used to test the approach against numerically exact benchmarks.

Since its theoretical conception [1] and the first experimental evidence of measurements on single-molecule junctions [2], molecular electronics has challenged theory for a proper description of response in open molecular systems far form equilibrium. Theoretical treatments are often based on a perturbative expansion in a small parameter, such as the strength of intra-molecular interactions or molecule-contact couplings. The former can be conveniently treated within the standard nonequilibrium Green function (NEGF) technique [3, 4], while the latter are handled at the nonequilibrium molecular limit [5] by many-body flavors of Green function (GF) methodology including pseudo-particles (PP) [6, 7] or Hubbard NEGF [8, 9] techniques. These two limits account for the majority of experimental measurements. For example, inelastic electron tunneling spectroscopy [10] is usually treated within NEGF [11, 12], while Coulomb blockade [13], single molecule strong coupling in plasmonic nanocavities [14] and coherent electron-nuclear dynamics [15] require many-body local analysis [16, 17].

In the absence of a small parameter or when molecule-lead correlations cannot be adequately described within perturbation theory, theoretical treatment is more involved. For example, this is the situation one encounters in describing Kondo physics in molecular junctions [18–24]. Theoretical methods for strongly correlated systems include dynamical mean field theory (DMFT) [7, 25], density matrix renormalization group (DMRG) technique [26, 27], scattering states-numerical renormalization group approach [28, 29], flow equations [30, 31], multilayer multiconfiguration time-dependent Hartree (ML-MCTDH) [32, 33], continuous time quantum Monte Carlo (CT-QMC) [34–36] and others. These methods are numerically demanding and are mostly limited to simple models. DMFT, which assumes only that correlations are local, is more general and is extensively used in simulations of strongly correlated materials (extended systems).

One way to account for nonlocal correlations in extended systems is the dual-fermion (DF) approach [38]. We note in passing that besides the DF many other studies extending DMFT beyond local correlations are

available in the literature. For a comprehensive review see Ref. 39 and references therein. Originally, the DF method was formulated for equilibrium systems [40, 41]. A nonequilibrium version of the method (DF-inspired superperturbation theory) was later proposed in Ref. 37 as a way to solve impurity/transport problems. An attractive feature of the latter formulation is its applicability in the absence of a small parameter. At the heart of the approach is *a reference system*, which includes the molecule and a finite number of states representing leads. Such finite problem can be solved exactly, though the system-lead couplings are then only an approximation of the original problem. DF introduces an auxiliary zero order Hamiltonian around which standard diagrammatics can be formulated. The resulting expansion accounts for the difference between the true system-lead hybridization and its approximation within the reference system (see Ref. 37).

Where the steady-state is of interest, the nonequilibrium DF approach of Ref. 37 requires significant numerical effort. Because only a few sites represent infinite baths in the reference system, the hybridization function differs significantly from the true one. Furthermore, the finite reference system necessarily yields periodic so-
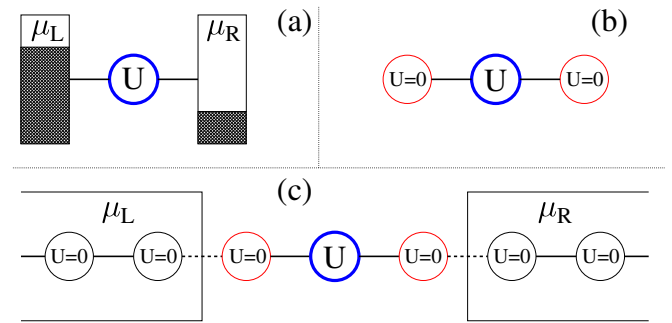

FIG. 1: Nonequilibrium junction model. Shown are (a) Anderson impurity model; (b) Reference system within original DF approach [37]; and (c) Reference system within auxiliary QME-DF approach.

lution, such that reaching the steady-state from the initially decoupled system and bath requires long time propagation.

We propose to utilize the solution of an auxiliary quantum master equation as a reference system for the DF approach in steady-state (compare Figs. 1b and c). The auxiliary QME yields a description of the hybridization and nonequilibrium state of the system which is much closer to the true solution than any finite reference system. Furthermore, time propagation is completely avoided. We note that the auxiliary QME has previously been used as a DMFT impurity solver [42, 43]. Here, we use it as a starting point for a more accurate DF impurity solver.

Nonequilibrium DF. In the nonequilibrium DF approach (for details see Ref. 37 and Supplemental Material [44]), one considers reduced dynamics of an open system with interactions confined to the molecular subspace and the effect of the leads entering via corresponding self-energies. The effective action on the Keldysh contour is [45]

$$S[d^*, d] = \sum_{1,2} d_1^* \left[G_0^{-1} - \Sigma^B \right]_{12} d_2 + S^{int}[d^*, d], \quad (1)$$

where $i = (m_i, \tau_i)$ $(i = 1, 2)$ is the index incorporating molecular orbital m_i and Keldysh contour variable τ_i, and the summation indicates sum over molecular orbitals and integral over the contour variables. $d_i^* = d_{m_i}^*(\tau_i)$ $(d_i = d_{m_i}(\tau_i))$ is the Grassmann variable corresponding to creation (annihilation) operator $\hat{d}_{m_i}^\dagger(\tau_i)$ $(\hat{d}_{m_i}(\tau_i))$ of an electron in orbital m_i in the Heisenberg picture [46]. G_0^{-1} is the inverse free GF [47]

$$\left[G_0^{-1} \right]_{12} \equiv \delta(\tau_1, \tau_2) \left[i \overrightarrow{\partial}_{\tau_1} \delta_{m_1, m_2} - H_{m_1 m_2}^0(\tau_1) \right] - \Sigma_{12}^{irr} \quad (2)$$

$$= \left[-i \overleftarrow{\partial}_{\tau_2} \delta_{m_1, m_2} - H_{m_1 m_2}^0(\tau_2) \right] \delta(\tau_1, \tau_2) - \Sigma_{12}^{irr},$$

and $\Sigma^B(\tau_1, \tau_2)$ is the self-energy due to coupling to contacts [61]

$$\Sigma_{m_1 m_2}^B(\tau_1, \tau_2) = \sum_{k \in B} V_{m_1 k} g_k(\tau_1, \tau_2) V_{k m_2}. \quad (3)$$

In Eqs. (2) and (3), $H_{m_1 m_2}^0(\tau)$ is the non-interacting part of the molecular Hamiltonian, $\Sigma_{m_1 m_2}^{irr}(\tau_1, \tau_2) \sim \delta(\tau_1, \tau_2)$ is the irregular self-energy, V_{mk} is the matrix element for electron transfer between molecular orbital m and contact state k, and $g_k(\tau_1, \tau_2) \equiv -i\langle T_c \hat{c}_k(\tau_1) \hat{c}_k^\dagger(\tau_2) \rangle$ is the GF of free electron in state k of the contacts. All intra-molecular interactions are within the (unspecified) contribution to the action, $S^{int}[d^*, d]$.

The DF approach is based on two important steps. First, one introduces an exactly solvable reference system with baths represented by a finite number of states. Its known action $\tilde{S}[d^*, d]$ has the same general form (1)

with true self-energy Σ^B substituted by its approximate representation $\tilde{\Sigma}^B$. The desired action S can then be written as

$$S[d^*, d] = \tilde{S}[d^*, d] + \sum_{1,2} d_1^* \left[\tilde{\Sigma}^B - \Sigma^B \right]_{12} d_2. \quad (4)$$

Second, direct application of standard diagrammatic expansion around the interacting reference system is not possible, because the Wick's theorem does not apply [48]. To resolve this, an artificial particle (*dual fermion*) is introduced which is used to unravel the term via the Hubbard-Stratonovich transformation [49]. Integrating out molecular fermions (d and d^*) and comparing the second order cumulant expansion of the resulting expression with the general form of action for dual fermions, $S^{DF}[f^*, f] = \sum_{1,2} f_1^* \left[(G_0^{DF})^{-1} - \Sigma^{DF} \right]_{12} f_2$, one gets

$$\left(G_0^{DF} \right)_{12}^{-1} = -g_{12}^{-1} - \sum_{3,4} g_{13}^{-1} \left[\tilde{\Sigma}^B - \Sigma^B \right]_{34}^{-1} g_{42}^{-1}, \quad (5)$$

$$\Sigma_{12}^{DF} = \sum_{3,4} \Gamma_{13;24} \left[G_0^{DF} \right]_{43}. \quad (6)$$

Here g_{12} and $\Gamma_{13;24}$ are the single-particle GF and the two-particle vertex of the reference system, respectively [4].

With $\left(G^{DF} \right) = \left[\left(G_0^{DF} \right)^{-1} - \Sigma^{DF} \right]^{-1}$ known, the single-particle GF of the molecule is obtained from

$$G = \left(\delta \Sigma^B \right)^{-1} + \left[g \, \delta \Sigma^B \right]^{-1} G^{DF} \left[\delta \Sigma^B \, g \right]^{-1}, \quad (7)$$

where $\delta \Sigma^B \equiv \tilde{\Sigma}^B - \Sigma^B$.

Auxiliary QME. The choice of reference system is arbitrary, but its ability to describe the physics reflects on the accuracy of the associated DF approach. In this sense a finite reference system (see Fig. 1b) may not be optimal: its inability to represent dissipation and inevitably periodic solution makes reaching the steady-state difficult. We propose using a reference with infinite leads, with the majority of lead states treated implicitly (integrated out) and a finite number included in an extended molecule-lead system (see Fig. 1c). Effectively, this complements choice of Ref. 37 with actual baths. We use a Markovian QME,

$$\frac{d\rho^S(t)}{dt} = -i\mathcal{L}\rho^S(t), \quad (8)$$

to simulate the extended system. Here, $\rho^S(t)$ is the extended system density operator and $\mathcal{L}$ is the Liouvillian. Our approach maintains all the advantages of Ref. 37 adding infinite baths, which results in a substantially more accurate and less numerically expensive computational scheme. Below, we focus on steady-state, where correlation functions depend on time differences, and work in the energy representation.

The nonequilibrium DF approach, Eqs. (5)-(6), requires single- and two-particle Green functions of the reference system as an input. To provide these we utilize the quantum regression relation [50]

$$\langle T_c \, \hat{A}(\tau_1) \, \hat{B}(\tau_2) \dots \hat{Z}(\tau_n)\rangle = \quad (9)$$
$$\mathrm{Tr}\big[\mathcal{O}_n \, \mathcal{U}(t_n, t_{n-1}) \dots \mathcal{O}_2 \, \mathcal{U}(t_2, t_1) \, \mathcal{O}_1 \, \mathcal{U}(t_1, 0) \, \rho^S(0)\big]$$

Here $\rho^S(0)$ is the steady-state density matrix of the extended system, $\mathcal{U}(t_i, t_{i-1})$ is the Liouville space evolution operator and times t_i are ordered so that $t_n > t_{n-1} > \dots > t_2 > t_1 > 0$. $\mathcal{O}_i$ is the Liouville space super-operator corresponding to one of operators $\hat{A} \dots \hat{Z}$ whose time is i-th in the ordering. It acts from the left (right) for the operator on the forward (backward) branch of the contour. The steady-state density matrix is found as a right eigenvector $|R_0 \gg$ corresponding to the Liouvillian eigenvalue $\lambda_0 = 0$. Using spectral decomposition of the Liouvillian, the evolution operator can be presented in its eigenbasis as

$$\mathcal{U}(t_i, t_{i-1}) = \sum_\gamma |R_\gamma \gg e^{-i\lambda_\gamma(t_i - t_{i-1})} \ll L_\gamma|. \quad (10)$$

For evaluation of single- and two-particle GFs, besides the $\mathcal{L}$ of Eq. (8) we will also need Liouvillians $\mathcal{L}^{(\pm 1)}$ and $\mathcal{L}^{(\pm 2)}$. These are evolution operator generators for Liouville space vectors $|S_1 S_2 \gg$ with different number N_S of electrons in states $|S_1\rangle$ and $|S_2\rangle$. For example, for $\mathcal{L}^{(+1)}$, $N_{S_1} = N_{S_2} + 1$ [62].

Using (10) in (9) yields expressions for the GFs of the reference system (see [44] for details). Once single- and two-particle GFs of the reference system are known, the vertex required in (6) is given by

$$\Gamma_{13;24} = \quad (11)$$
$$\sum_{\substack{1',2'\\3',4'}} g_{11'}^{-1} g_{33'}^{-1} \big[g_{1'3';2'4'}^{(2)} - g_{1'2'} g_{3'4'} + g_{1'4'} g_{3'2'}\big] g_{2'2}^{-1} g_{4'4}^{-1}.$$

Below we consider extended systems of size small enough that exact diagonalization can be employed. For larger systems more advanced methods (e.g. matrix product states [51]) may be used.

Model. We apply the QME-DF method to the Anderson impurity model: junction is constructed from quantum dot coupled to two paramagnetic leads each at its own equilibrium (see Fig. 1a). The Hamiltonian is

$$\hat{H} = \hat{H}_M + \sum_{K=L,R} \big(\hat{H}_K + \hat{V}_{MK}\big), \quad (12)$$

where $\hat{H}_M = \sum_{\sigma=\uparrow,\downarrow} \epsilon_0 \hat{d}_\sigma^\dagger \hat{d}_\sigma + U\hat{n}_\uparrow \hat{n}_\downarrow$ and $\hat{H}_K = \sum_{k \in K} \sum_{\sigma=\uparrow,\downarrow} \epsilon_k \hat{c}_{k\sigma}^\dagger \hat{c}_{k\sigma}$ are Hamiltonians of the quantum dot and contact K and $\hat{V}_{MK} = \sum_{k \in K} \sum_{\sigma=\uparrow,\downarrow} \big(V_k \hat{d}_\sigma^\dagger \hat{c}_{k\sigma} + H.c.\big)$ describes electron transfer between the dot and contact. The $\hat{d}_\sigma^\dagger$

$(\hat{d}_\sigma)$ and $\hat{c}_{k\sigma}^\dagger$ $(\hat{c}_{k\sigma})$ creates (annihilates) electron of spin σ on the dot and in state k of the contacts, respectively. U is the Coulomb repulsion and $\hat{n}_\sigma = \hat{d}_\sigma^\dagger \hat{d}_\sigma$.

Using Eq. (7) we calculate the GF

$$G_\sigma(\tau_1, \tau_2) = -i\langle T_c \, \hat{d}_\sigma(\tau_1) \, \hat{d}_\sigma^\dagger(\tau_2)\rangle, \quad (13)$$

and use it to evaluate the level population n_σ, spectral function $A_\sigma(E)$, and current $I_L = -I_R$ [52] in steady-state

$$n_\sigma = -i \int \frac{dE}{2\pi} G_\sigma^<(E); \quad A_\sigma(E) = -\frac{1}{\pi}\mathrm{Im}\, G_\sigma^r(E),$$
$$I_K = \sum_\sigma \int \frac{dE}{2\pi} \big(\Sigma_K^<(E) G_\sigma^>(E) - \Sigma_K^>(E) G_\sigma^<(E)\big).$$
$$(14)$$

Here $<, >$ and r are respectively lesser, greater and retarded projections of the GF. $\Sigma_K^{\gtrless}(E)$ is the greater/lesser projection of the self-energy due to lead $K \in \{L, R\}$. Following Ref. 53, we model the leads as semi-infinite tight-binding chains with on-site energies ϵ_K and hopping parameter t_K $(K = L, R)$; the electron hopping between the quantum dot and chain is t_{MK}.

Numerical results. We compare the QME-DF approach to the Anderson impurity model with the original nonequilibrium DF scheme and with numerically exact tdDMRG and CT-QMC calculations. The former were performed using ALPS-MPS [54, 55], while the latter utilize the Inchworm algorithm introduced in Ref. 34. The units are set by the maximum total escape rate, $\Gamma_0 = 2\, t_{ML}^2/t_L + 2\, t_{MR}^2/t_R$: in particular, we employ units of energy, $E_0 = \Gamma_0$, time $t_0 = \hbar/E_0$, voltage $V_0 = E_0/|e|$ and current $I_0 = |e|E_0/\hbar$. We show two flavors of the QME-DF results: zero order, where one neglects self-energy Σ^{DF}, and first order, where the self-energy is evaluated using Eq. (6).

Unless stated otherwise, the parameters are as follows: $U = 5E_0$, $\epsilon_0 = -U/2$, $t_{ML} = t_{MR} = 0.79E_0$ and $t_L = t_R = 2.5E_0$. The positions of the on-site energies in the leads, ϵ_K, are given by the corresponding chemical potentials μ_K. The Fermi energy $E_F = 0$ is taken as the origin, and bias is assume dot be applied symmetrically such that $\mu_{L/R} = E_F \pm |e|V_{sd}/2$. The temperature is zero. The QME-DF simulations are performed on energy grid spanning range from $-12.5E_0$ to $12.5E_0$ with step $0.0125E_0$.

Figure 2a shows QME-DF level populations $n_\uparrow = n_\downarrow \equiv n_0$ under a bias $V_{sd} = 2.5V_0$, at several level positions ϵ_0, evaluated directly in steady-state. In contrast, the inset of Fig. 2a displays the corresponding time propagation of the population following a molecule-lead coupling quench simulation of Ref. 37, illustrating the difficulty of reaching steady-state within the orginial nonequilibirum DF approach. Figure 2b shows the current at identical parameters. In both panels of Figure 2, we compare the zero (DF0, dashed line) with the first (DF, solid line) order
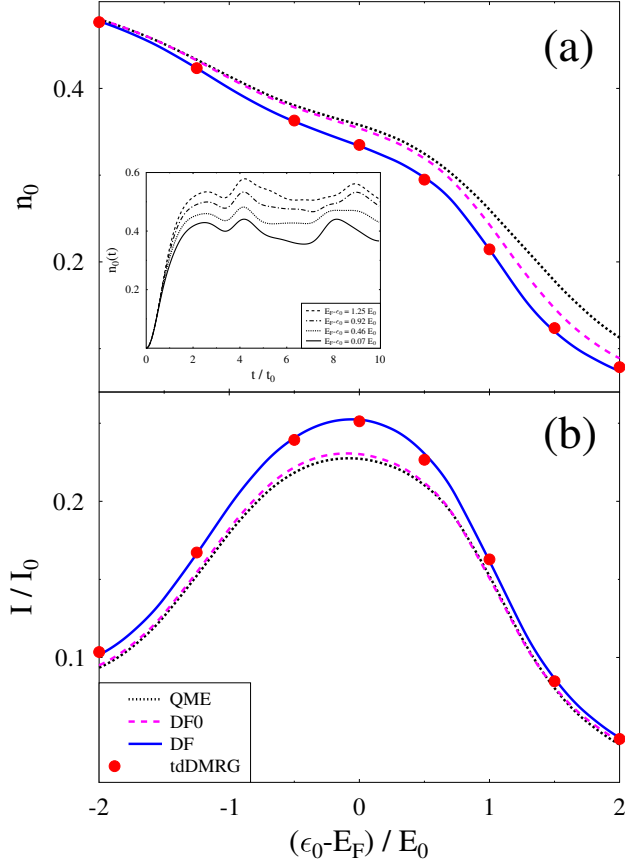
FIG. 2: (Color online) Steady-state transport characteristics vs. gate voltage at fixed bias. Shown are (a) population and (b) current vs. level position, as calculated from auxiliary QME (dotted line); and zero (dashed line) and first (solid line) order QME-DF approaches. Circles (red) represent results of numerically exact tdDMRG simulations. The inset in panel (a) shows the results of the original nonequilibrium DF simulation, where at $t = 0$ coupling between system and contacts is switched on for several level positions.
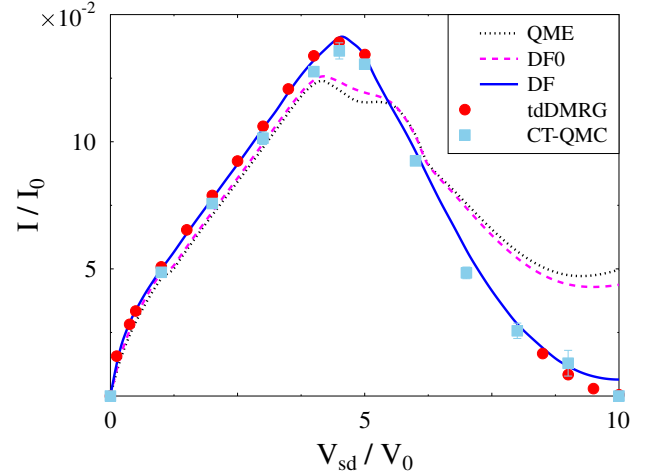

FIG. 3: (Color online) Current voltage characteristics. We show the auxiliary QME (dotted line), zero (dashed line) and first (solid line) order QME-DF approaches. For comparison, circles and squares represent respectively tdDMRG and CT-QMC results.

QME-DF approach, the auxiliary QME (QME, dotted line) and numerically exact tdDMRG results at $t = 8t_0$. The first order QME-DF approach is quite accurate in predicting both level populations and currents, while being substantially less expensive numerically than the original DF formulation and having the added advantage of direct access to steady-state.

In Figure 3, we consider current-voltage characteristics in the particle-hole symmetric case, within the auxiliary QME (dotted line), the zero (dashed line) and first (solid line) order QME-DF. The latter is quite close to numerically exact tdDMRG (circles) and CT-QMC calculations (squares). Interestingly, the first order QME-DF calculation with three auxiliary sites yields result similar to a much more expensive six-site QME simulation (compare with Fig. 3 of Ref. 43).

Finally, we consider spectral function: Fig. 4a shows results of equilibrium ($V_{sd} = 0$, solid line) and nonequilibrium ($V_{sd} = 2.5V_0$, dtted line) simulations; Fig. 4b shows the spectral function varying with bias. At low biases equilibrium Kondo peak splits and follows corresponding chemical potentials, while higher biases destroy the correlation. Similar results were obtained in Refs. 28, 56–59. Note that results in Fig. 4 are only qualitative representation of true Kondo physics, but equilibrium DF studies, e.g., Ref. 40, have shown that accurate results in the correlated regime can be obtained efficiently by accounting for higher order diagrams.

Conclusion. The nonequilibrium dual fermion approach introduced originally in Ref. 37 is a promising method for simulating strongly correlated open systems. Contrary to usual diagrammatic expansions in small interaction (e.g., intra-system interaction in NEGF or system-bath couplings in PP- or Hubbard NEGF), the method can treat systems with no small parameter by expanding around an exactly solvable reference system. The choice of a finite reference system in the original DF formulation cannot properly describe bath induced dissipation and results in periodic dynamics, which, together with the necessity to consider time propagation starting from a decoupled initial state, complicates reaching steady-state.

We proposed complementing finite reference system with infinite Markovian baths and use auxiliary quantum master equation to solve the reference problem. We argued that the approach is advantageous in treating the steady-states because it yields reference system which is much closer to the true nonequilibrium state than that in the original formulation. Also, infinite size of the modified reference system results in more accurate descrip-
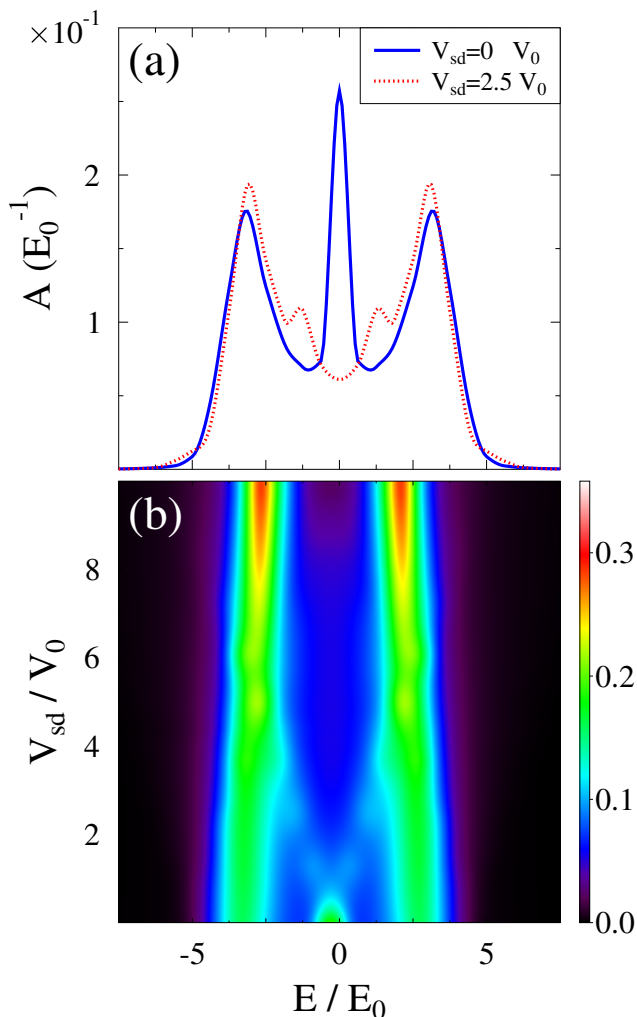
FIG. 4: (Color online) Spectral function of Anderson impurity model. Shown are results of QME-DF simulations for (a) The spectral function of the unbiased ($V_{sd} = 0$, solid line) and biased junction ($V_d/V_0 = 2.5$, dotted line); and (b) The spectral function vs. energy and applied bias.

tion of bath induced dissipation. Finally, the approach allows to avoid long time propagations necessary to reach steady-state solution in the original formulation.

For the Anderson impurity model, we tested our approach by comparing QME-DF simulations with numerically exact tdDMRG and CT-QMC results. This showed that the new scheme is both accurate and inexpensive. Further development of the method and its application to realistic systems is a goal for future research.

* Electronic address: migalperin@ucsd.edu

[1] A. Aviram and M. A. Ratner, Chem. Phys. Lett. **29**, 277 (1974).
[2] M. A. Reed, C. Zhou, C. J. Muller, T. P. Burgin, and J. M. Tour, Science **278**, 252 (1997).
[3] H. Haug and A.-P. Jauho, *Quantum Kinetics in Transport and Optics of Semiconductors* (Springer, Berlin Heidelberg, 2008), second, substantially revised edition ed.
[4] G. Stefanucci and R. van Leeuwen, *Nonequilibrium Many-Body Theory of Quantum Systems. A Modern Introduction.* (Cambridge University Press, 2013).
[5] A. J. White, M. A. Ochoa, and M. Galperin, Journal of Physical Chemistry C **118**, 11159 (2014).
[6] J. H. Oh, D. Ahn, and V. Bubanja, Phys. Rev. B **83**, 205302 (2011).
[7] H. Aoki, N. Tsuji, M. Eckstein, M. Kollar, T. Oka, and P. Werner, Rev. Mod. Phys. **86**, 779 (2014).
[8] F. Chen, M. A. Ochoa, and M. Galperin, J. Chem. Phys. **146**, 092301 (2017).
[9] K. Miwa, F. Chen, and M. Galperin, Scientific Reports **7**, 9735 (2017).
[10] W. Wang, T. Lee, I. Kretzschmar, and M. A. Reed, Nano Letters **4**, 643 (2004).
[11] T. Frederiksen, M. Paulsson, M. Brandbyge, and A.-P. Jauho, Phys. Rev. B **75**, 205413 (2007).
[12] R. Avriller and T. Frederiksen, Phys. Rev. B **86**, 155411 (2012).
[13] M. Poot, E. Osorio, K. O'Neill, J. M. Thijssen, D. Vanmaekelbergh, C. A. v. Walree, L. W. Jenneskens, and H. S. J. v. d. Zant, Nano Letters **6**, 1031 (2006).
[14] R. Chikkaraddy, B. de Nijs, F. Benz, S. J. Barrow, O. A. Scherman, E. Rosta, A. Demetriadou, P. Fox, O. Hess, and J. J. Baumberg, Nature **535**, 127 (2016).
[15] J. Repp, P. Liljeroth, and G. Meyer, Nature Physics **6**, 975 (2010).
[16] J. S. Seldenthuis, H. S. J. van der Zant, M. A. Ratner, and J. M. Thijssen, ACS Nano **2**, 1445 (2008).
[17] A. J. White, B. D. Fainberg, and M. Galperin, J. Phys. Chem. Lett. **3**, 2738 (2012).
[18] J. Park, A. N. Pasupathy, J. I. Goldsmith, C. Chang, Y. Yaish, J. R. Petta, M. Rinkoski, J. P. Sethna, H. D. Abruña, P. L. McEuen, et al., Nature **417**, 722 (2002).
[19] W. Liang, M. P. Shores, M. Bockrath, J. R. Long, and H. Park, Nature **417**, 725 (2002).
[20] L. H. Yu, Z. K. Keane, J. W. Ciszek, L. Cheng, J. M. Tour, T. Baruah, M. R. Pederson, and D. Natelson, Phys. Rev. Lett. **95**, 256803 (2005).
[21] E. A. Osorio, K. O'Neill, M. Wegewijs, N. Stuhr-Hansen, J. Paaske, T. Bjrnholm, and H. S. J. van der Zant, Nano Letters **7**, 3336 (2007).
[22] J. J. Parks, A. R. Champagne, T. A. Costi, W. W. Shum, A. N. Pasupathy, E. Neuscamman, S. Flores-Torres, P. S. Cornaglia, A. A. Aligia, C. A. Balseiro, et al., Science **328**, 1370 (2010).
[23] S. Wagner, F. Kisslinger, S. Ballmann, F. Schramm, R. Chandrasekar, T. Bodenstein, O. Fuhr, D. Secker, K. Fink, M. Ruben, et al., Nature Nanotechnology **8**, 575 (2013).
[24] D. Rakhmilevitch and O. Tal, Beilstein Journal of Nanotechnology **6**, 2417 (2015).
[25] V. Anisimov and Y. Izyumov, *Electronic Structure of*

Strongly Correlated Materials (Springer, 2010).

[26] U. Schollwöck, Rev. Mod. Phys. **77**, 259 (2005).

[27] U. Schollwöck, Annals of Physics **326**, 96 (2011).

[28] F. B. Anders, Phys. Rev. Lett. **101**, 066804 (2008), URL http://link.aps.org/abstract/PRL/v101/e066804.

[29] S. Schmitt and F. B. Anders, Phys. Rev. B **81**, 165106 (2010).

[30] F. Wegner, Annalen der Physik **506**, 77 (1994).

[31] S. Kehrein, *The Flow Equation Approach to Many-Particle Systems*, vol. 217 of *Springer Tracts in Modern Physics* (Springer-Verlag, 2006).

[32] H. Wang and M. Thoss, J. Chem. Phys. **131**, 024114 (2009).

[33] H. Wang and M. Thoss, Chemical Physics **509**, 13 (2018).

[34] G. Cohen, E. Gull, D. R. Reichman, and A. J. Millis, Phys. Rev. Lett. **115**, 266802 (2015).

[35] A. E. Antipov, Q. Dong, J. Kleinhenz, G. Cohen, and E. Gull, Phys. Rev. B **95**, 085144 (2017).

[36] M. Ridley, V. N. Singh, E. Gull, and G. Cohen, Phys. Rev. B **97**, 115109 (2018).

[37] C. Jung, A. Lieder, S. Brener, H. Hafermann, B. Baxevanis, A. Chudnovskiy, A. Rubtsov, M. Katsnelson, and A. Lichtenstein, Annalen der Physik **524**, 49 (2012).

[38] A. N. Rubtsov, M. I. Katsnelson, and A. I. Lichtenstein, Phys. Rev. B **77**, 033101 (2008).

[39] G. Rohringer, H. Hafermann, A. Toschi, A. A. Katanin, A. E. Antipov, M. I. Katsnelson, A. I. Lichtenstein, A. N. Rubtsov, and K. Held, Rev. Mod. Phys. **90**, 025003 (2018), ISSN 0034-6861, 1539-0756, URL https://link.aps.org/doi/10.1103/RevModPhys.90.025003.

[40] Hafermann, H., Jung, C., Brener, S., Katsnelson, M. I., Rubtsov, A. N., and Lichtenstein, A. I., EPL **85**, 27007 (2009).

[41] A. E. Antipov, J. P. F. LeBlanc, and E. Gull, Physics Procedia **68**, 43 (2015).

[42] E. Arrigoni, M. Knap, and W. von der Linden, Phys. Rev. Lett. **110**, 086403 (2013).

[43] A. Dorda, M. Nuss, W. von der Linden, and E. Arrigoni, Phys. Rev. B **89**, 165105 (2014).

[44] F. Chen, G. Cohen, and M. Galperin, Phys. Rev. Lett. **this letter** (2018).

[45] A. Kamenev, *Field Theory of Non-Equilibrium Systems* (Cambridge University Press, 2011).

[46] J. W. Negele and H. Orland, *Quantum Many-Particle Systems*, vol. 68 (Addison-Wesley Publishing Company, Redwood City, California, 1988).

[47] M. Wagner, Phys. Rev. B **44**, 6104 (1991).

[48] A. L. Fetter and J. D. Walecka, *Quantum Theory of Many-Particle Systems* (McGraw-Hill Book Company, 1971).

[49] P. Coleman, *Introduction to Many-Body Physics* (Cambridge University Press, 2015).

[50] H.-P. Breuer and F. Petruccione, *The Theory of Open Quantum Systems* (Oxford University Press, 2003).

[51] A. Dorda, M. Ganahl, H. G. Evertz, W. von der Linden, and E. Arrigoni, Phys. Rev. B **92**, 125145 (2015).

[52] A.-P. Jauho, N. S. Wingreen, and Y. Meir, Phys. Rev. B **50**, 5528 (1994).

[53] D. M. Newns, Physical Review **178**, 1123 (1969).

[54] B. Bauer, L. D. Carr, H. G. Evertz, A. Feiguin, J. Freire, S. Fuchs, L. Gamper, J. Gukelberger, E. Gull, S. Guertler, et al., p. 35 (2011).

[55] M. Dolfi, B. Bauer, S. Keller, A. Kosenkov, T. Ewart, A. Kantian, T. Giamarchi, and M. Troyer, Computer Physics Communications **185**, 3430 (2014).

[56] Y. Meir, N. S. Wingreen, and P. A. Lee, Phys. Rev. Lett. **70**, 2601 (1993).

[57] N. S. Wingreen and Y. Meir, Phys. Rev. B **49**, 11040 (1994).

[58] N. Sivan and N. S. Wingreen, Physical Review B **54**, 11622 (1996).

[59] G. Cohen, E. Gull, D. R. Reichman, and A. J. Millis, Phys. Rev. Lett. **112**, 146802 (2014), URL https://link.aps.org/doi/10.1103/PhysRevLett.112.146802.

[60] M. Leijnse and M. R. Wegewijs, Physical Review B **78**, 235424 (2008).

[61] Note that contrary to Ref. 37 which used Δ to indicate hybridization function, here we follow traditional quantum transport notation where self-energy due to coupling to contacts is indicated with Σ.

[62] Note, constructing the Liouvillians is helped by conservation of $N_{S_1} - N_{S_2}$ during evolution. Other symmetries (charge, spin) may help in understanding block structure within the Liouvillians [60].